THE JOURNAL OF BIOLOGICAL CHEMISTRY VOL. 285, NO. 13, pp. 9740–9748, March 26, 2010

Tobacco Calcium-dependent Protein Kinases Are Differentially Phosphorylated *in Vivo* as Part of a Kinase Cascade That Regulates Stress Response*[S]

Received for publication, August 4, 2009, and in revised form, January 29, 2010 Published, JBC Papers in Press, January 29, 2010, DOI 10.1074/jbc.M109.052126

Claus-Peter Witte[‡], Nana Keinath[§], Ullrich Dubiella[‡], Raphael Demoulière[§], Anindita Seal[¶], and Tina Romeis[‡1]

From the [‡]Department of Plant Biochemistry, Institute for Biology, Freie Universität Berlin, Königin-Luise-Strasse 12-16, 14195 Berlin, Germany, the [§]Department of Plant Microbe Interactions, Max Planck Institute for Plant Breeding Research, Carl-von-Linné-Weg 10, 50935 Cologne, Germany, and the [¶]Department of Biotechnology, West Bengal University of Technology BF-142, Sector I, Salt Lake, Calcutta 700064, India

In vivo **phosphorylation sites of the tobacco calcium-dependent protein kinases NtCDPK2 and NtCDPK3 were determined in response to biotic or abiotic stress. Stress-inducible phosphorylation was exclusively located in the variable N termini, where both kinases were phosphorylated differentially despite 91% overall sequence identity. In NtCDPK2, serine 40 and threonine 65 were phosphorylated within 2 min after stress. Whereas Thr^{65} is subjected to intra-molecular *in vivo* autophosphorylation, Ser^{40} represents a target for a regulatory upstream protein kinase, and correct NtCDPK2 membrane localization is required for Ser^{40} phosphorylation. NtCDPK3 is phosphorylated at least at two sites in the N terminus by upstream kinase(s) upon stress stimulus, first at Ser^{54}, a site not present in NtCDPK2, and also at a second undetermined site not identical to Ser^{40}. Domain swap experiments established that differential phosphorylation of both kinases is exclusively determined by the respective N termini. A cell death-inducing response was only observed upon expression of a truncated variant lacking the junction and calcium-binding domain of NtCDPK2 (VK2). This response required protein kinase activity and was reduced when subcellular membrane localization was disturbed by a mutation in the myristoylation and palmitoylation site. Our data indicate that CDPKs are integrated in stress-dependent protein kinase signaling cascades, and regulation of CDPK function in response to *in vivo* stimulation is dependent on its membrane localization.**

Calcium-dependent protein kinases (CDPKs)[2] form a gene family of 34 and 29 members in *Arabidopsis thaliana* and rice, respectively. They possess a conserved modular structure of four domains (VKJC): an N-terminal variable domain (V), which for many isoforms contains a myristoylation and palmitoylation motif mediating membrane localization; a serine/threonine protein kinase domain (K); an autoinhibitory junction peptide (J); and a calcium-sensing calmodulin-like domain (C) at the C terminus (1). These structural features as well as published biochemical and functional data suggest that the regulatory switch for CDPK *in vivo* activation includes (i) the binding of calcium leading to the release of the autoinhibitory domain from the active site, (ii) CDPK protein (auto)phosphorylation, and (iii) specific subcellular localization (2–6).

CDPKs have been associated with the regulation of diverse processes of plant growth and development, nutrient primary metabolism, and signaling in biotic and abiotic stress responses and water/ion transport (7–9). Only recently, the analysis of genetic knock-out mutants in *Arabidopsis* allowed the assignment of a biological function in abscisic acid signaling, stomatal aperture, and salt stress tolerance to *Arabidopsis* CPK4 (calcium-dependent protein kinase 4) and CPK11 (10), CPK3 and CPK6 (11), and CPK23 (12), respectively. However, none of these studies addressed the biochemical mechanism of how the CDPK enzyme itself is regulated by (auto)phosphorylation *in planta*.

In vitro autophosphorylation of CDPKs using recombinant or purified enzymes was observed for almost all CDPKs studied so far. The corresponding *in vitro* autophosphorylation sites (P-sites) have been mapped for several enzymes (13–16) and were found with high frequency in the variable N termini (17). It has not yet been experimentally addressed whether CDPK autokinase reactions follow an intramolecular (unimolecular: kinase and P-site on the same polypeptide) or intermolecular (bimolecular: kinase and P-site on different polypeptide) mechanism or both. *In vivo* P-sites of CDPKs have not been mapped comprehensively, although some P-sites of *Arabidopsis* CDPKs have been identified in general plant phosphoproteomics analyses (18, 19). For NtCDPK2, one *in vivo* P-site has been described (20). The *in vivo* relevance and function of CDPK phosphorylation remains to be shown. It has been proposed that CDPK phosphorylation is required for enzyme activation (21–23). For CDPKs from soybean and groundnut, it was demonstrated that *in vitro* autophosphorylation did not relieve kinase activity from calcium dependence (22, 24) as

* This work was supported by a European Molecular Biology Organization long term fellowship (to C.-P. W.) and by Deutsche Forschungsgemeinschaft Research Consortia SFB 635 and SPP1212 (to T. R.).

[S] The on-line version of this article (available at http://www.jbc.org) contains supplemental Tables S1–S3 and Figs. S1–S7.

[1] To whom correspondence should be addressed. Tel.: 49-30-83853123; Fax: 49-30-83853372; E-mail: romeis@zedat.fu-berlin.de.

[2] The abbreviations used are: CDPK, calcium-dependent protein kinase; P-site, phosphorylation site; auto-P-site, autophosphorylation site; HA, peptide from hemagglutinin protein; Myc, peptide from human c-Myc protein; peptide T5-6, joined tryptic peptides number 5 and 6 (counting from the N terminus); VK2, variable and kinase domain only of NtCDPK2; VK2-AA, NtCDPK2-VK variant with S40A and T65A mutation; VK2-DD, NtCDPK2-VK variant with S40D and T65D mutation; VK3, variable and kinase domain only of NtCDPK3; MS, mass spectrometry.

observed for mammalian calmodulin-dependent kinase II (25) or calmodulin-dependent kinase VI (26).

CDPK isoforms from tobacco (*Nicotiana tabacum*) were shown to participate in plant defense signaling. Treatment of tobacco plants or cell cultures containing the *Cf-9* (*Cladosporium fulvum* resistance gene 9) disease resistance gene from tomato with fungal pathogen-derived AVR9 (*C. fulvum* avirulence gene 9) peptide resulted in a rapid phosphorylation and activation of NtCDPK2 within a few minutes after elicitation (21, 27). Transient loss-of-function studies in *Nicotiana benthamiana* showed that plants silenced for the NtCDPK2 subfamily by virus-induced gene silencing were compromised in the induction of AVR9/CF-9-dependent hypersensitive response-like cell death symptoms (21). In complementary gain-of-function experiments, the ectopic expression of a truncated NtCDPK2-VK (VK2) variant lacking its regulatory junction- and calcium-binding domains triggered enhanced stress responses upon a mild hypo-osmotic shock (28).

Here we present a detailed analysis of stress-dependent phosphorylation of NtCDPK2 and NtCDPK3 proteins *in vivo*. Transient expression in *N. benthamiana*, rapid StrepII tag-mediated purification, and quadrupole time-of-flight mass spectrometry analyses were coupled with site-directed mutagenesis approaches to map phosphorylated amino acids, to study the time course and hierarchical order of phosphorylations, and to further characterize the phosphorylations. P-sites of both NtCDPKs were found to reside mainly in the variable N termini. Inter- and intramolecular autophosphorylation events as well as phosphorylations catalyzed by other kinases were identified, the latter requiring an intact myristoylation and palmitoylation motif. Our data demonstrate that CDPKs are integrated in protein kinase signaling cascades. Ectopically expressed in *N. benthamiana*, P-site variants still triggered a cell death response when introduced into VK2. Membrane localization of the enzyme was required for this response.

EXPERIMENTAL PROCEDURES

Cloning and Constructs—Clones for NtCDPK2 full-length constructs with C-terminal HA-Strep tag for plant expression and His tag for expression in *Escherichia coli* were described previously (14, 20). A triple-Myc-tagged NtCDPK2 construct was also described as well as CDPK silencing and the corresponding construct (21). The VK2 construct (amino acids 1–375) used in this study was generated by PCR with primers 3 and 5 (supplemental Table S1) using a full-length NtCDPK2 clone as template and cloned into pXCS-HAStrep (20) via the EcoRI and XmaI sites. To prevent bacterial expression, the internal MfeI-NcoI fragment of the VK2 cDNA was exchanged against the corresponding genomic fragment containing the first two NtCDPK2 introns. The NtCDPK3 construct was amplified with primers 3 and 271 (supplemental Table S1) and cloned into pXCS-HAStrep using the EcoRI and XmaI sites. The VK3 construct (amino acids 1–377) was generated by PCR using primers 3 and 296 and cloned into pXCS-HAStrep using the EcoRI and XmaI sites. Because this construct was toxic to the agrobacteria, two introns amplified from genomic tobacco DNA with primers 344 and 345 were cloned into the cDNA using the MfeI and NcoI restriction sites present in the NtCDPK3 coding sequence. Site-directed mutagenesis was performed according to Ref. 29. The PEST domain deletions (amino acids 27–42) were introduced by overlap PCR (30). N-terminal domain swap constructs were generated by mutually exchanging an EcoRI-DraI fragment coding for the complete N terminus and part of the kinase domain between NtCDPK2 and NtCDPK3 (in pXCS-HAStrep). Within the exchanged part of the kinase domain, all amino acids are identical between both kinases. Supplemental Table S1 lists all primers used in this study.

CDPK Expression, Protein Purification, and Analysis—Tagged NtCDPK enzymes were transiently expressed in *N. benthamiana* as described previously (20). For the analysis of phosphorylation-dependent mobility shifts, leaves expressing the corresponding kinase constructs were exposed to hypo-osmotic stress by infiltration of water with a syringe (or a cantharidin solution of 30 μM where indicated), and leaf discs of 15 mm diameter were cut at defined time points after infiltration. Leaf discs were immediately frozen in liquid nitrogen, placed into a 2-ml microcentrifuge tube containing a steel bead ($d = 3$ mm), and ground frozen in a Retsch MM300 mill (60 s; frequency 30 s^{-1}). The ground material was thawed while slowly moving on a vortex in 400 μl of extraction buffer A (50 mM Tris-HCl, pH 7.5, 5 mM EGTA, 5 mM EDTA, 5 mM dithiothreitol, 0.2 mM 4-(2-aminoethyl)benzenesulfonyl fluoride hydrochloride, 1 μg/ml leupeptin, 1 μg/ml aprotinin, protease inhibitor mixture, (diluted 1:500; Sigma P9599), 10 mM sodium fluoride (NaF), 10 mM sodium orthovanadate (Na_3VO_4), 10 mM β-glycerol phosphate, phosphatase inhibitor mixture (diluted 1:500; Sigma P2850)). After centrifugation at 21,000 $\times$ *g* (4 °C, 15 min), the supernatant was discarded, and the pellet was resuspended using a cooled sonication bath in 100–200 μl of extraction buffer B (25 mM Tris, pH 7.5, 2 mM dithiothreitol, 0.2 mM 4-(2-aminoethyl)benzenesulfonyl fluoride hydrochloride, 1 μg/ml leupeptin, 1 μg/ml aprotinin, protease inhibitor mixture (diluted 1:500), 5 mM NaF, 5 mM Na_3VO_4, 5 mM β-glycerol-phosphate, phosphatase inhibitor mixture (diluted 1:500), and 0.5% Triton X-100). Following centrifugation for 5 min (4 °C, 21,000 $\times$ *g*), 10 mM $MgCl_2$, 0.4 mM $CaCl_2$, and electrophoresis loading buffer were added to the supernatants. The addition of Mg^{2+} and Ca^{2+} saturates the metal chelators of extraction buffer B and avoids smiling effects of CDPK bands on Western blots. Electrophoresis and Western blot analyses were performed as described (20), except gels were run for an extended time period to achieve highest separation to distinguish differentially phosphorylated NtCDPK signals.

Separation of microsomal fractions and supernatants for the analysis of myristoylation and palmitoylation mutants was achieved by ultracentrifugation of the extract obtained in buffer A in a Beckman TLA 120.1 rotor at 220,000 $\times$ *g* for 30 min (4 °C). The pellet was resuspended in extraction buffer B by sonication and centrifuged again at 20,000 $\times$ *g* for 10 min.

For *in vitro* kinase reactions, 20 μl of enzyme affinity purified from leaves was mixed with 4 μl of water and 6 μl of 5$\times$ kinase buffer with or without ATP (200 mM HEPES, pH 7.5, 0.5 mM $CaCl_2$, 50 mM $MgCl_2$, 50 mM ATP or water) and incubated for 15 min at 30 °C. The reaction was stopped by adding 15 μl of 3$\times$ SDS-loading buffer.

Mass Spectrometry and Site-directed Mutagenesis—NtCDPK2 and NtCDPK3 protein purification from plant material for mass spectrometry (MS) analysis was performed as described (20). The isolation of NtCDPK2 from *E. coli* was carried out according to Glinski *et al.* (14). Mass spectra were scanned manually for the presence of potential phosphopeptides. Candidate peptides were analyzed by tandem MS to verify and map the phosphorylated amino acid. In an alternative approach, tandem MS analysis was performed for all peptides that contain a serine or threonine, taking into account one or two possible phosphorylations. The resulting data were compared manually to spectra from the non-phosphorylated peptides, where available, or to a theoretical prediction of fragment ions.

Autophosphorylation sites in kinases isolated from leaves were identified by comparing spectra of catalytically inactive NtCDPK2 and NtCDPK3 variants (D241A and D238A mutants, respectively) with spectra of the corresponding wild-type forms. In order to confirm autophosphorylation sites, His-tagged NtCDPK2 was expressed in *E. coli* and purified as described (14). The isolated recombinant enzyme was subjected to in-gel tryptic digest and quadrupole time-of-flight MS analysis. Previous *in vitro* incubation with ATP was not necessary because NtCDPK2 autophosphorylated during the bacterial expression. NtCDPK3 could not be expressed in *E. coli*, probably because it was toxic to the bacteria (also observed for PiCDPK2 (31)). P-sites found in NtCDPK2 expressed in *E. coli* that were absent in kinase-inactive mutants expressed *in planta* represent intramolecular auto-P-sites. Those P-sites found in both types of material are intermolecular auto-P-sites, although they may additionally also be phosphorylated by an intramolecular mechanism.

In cases where tandem MS analysis could not resolve the site of phosphorylation in a peptide, variants of NtCDPK2 with alanine substitutions of possible P-sites were subjected to MS analyses. The following variants were analyzed: S18A, S20A, S97A, T102A, S97A/T102A, and S104A. Semiquantitative evaluation of mass spectra to determine inducibility of phosphorylation by stress was performed by comparing ratios of phosphorylated peptide signals with total peptide (phosphorylated and non-phosphorylated) signals before and after stress.

Phenotypic Analysis of VK Constructs—The first fully expanded leaf on 3–4-week-old *N. benthamiana* plants was infiltrated with one of the following constructs: VK2, VK2-D241A (kinase inactive), VK2-G2A, VK2-AA (S40A/T65A), and VK2-DD (S40D/T65D). Agrobacteria carrying the respective kinase constructs at an $A_{600\ nm}$ of 0.2 were mixed with a concentrated solution of agrobacteria carrying the p19 silencing suppressor from tomato bushy stunt virus (32) reaching a final optical density of 0.3 for the mixture. Infiltration of this mixture was carried out in the evening, and plants were placed in a long day (16 h of light) growth chamber with strong lighting (300 microeinsteins $m^{-2}\,s^{-1}$) on the following day. One leaf disc was taken on day 2 as control for protein expression assayed by Western blot. On day 3, the developing cell death phenotype was assessed by documenting autofluorescence with a macroscope (Leica Z16APOA) equipped with a UV lamp and a long pass green fluorescent protein filter (I3) and a Leica DSC420C camera. Relative cell death was quantified by using the histogram function of Adobe Photoshop. For each image, the sum of pixels in the green channel with brightness of 20 or above was divided by the total number of pixels in this channel. Areas where the infiltration process had damaged the leaf were excluded. The resulting ratios were multiplied by 1000, and mean and S.D. values were calculated. Statistical significance was evaluated using an analysis of variance coupled with a Newman-Keuls post-test.

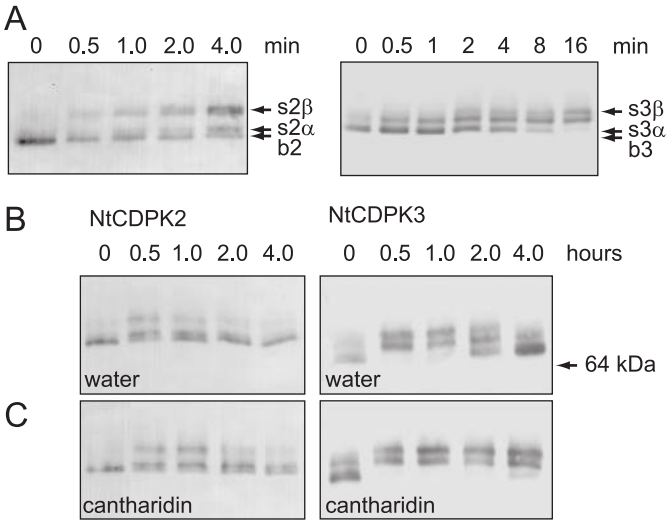

FIGURE 1. **Kinetics of stimulus-dependent NtCDPK2 and NtCDPK3 phosphorylation and effect of cantharidin visualized by electrophoretic mobility shifts.** *A*, Western blot of rapid phosphorylation kinetics for NtCDPK2 (*left*) and NtCDPK3 (*right*) detected using Strep-Tactin-alkaline phosphatase conjugate. The non-phosphorylated forms are labeled with *b2* and *b3*, and the phosphorylated forms are labeled with *s2α* and *s3α* for the smaller mobility shift and *s2β* and *3β* for the larger mobility shift, respectively. Shown is long term phosphorylation and dephosphorylation kinetics (Western blot) of NtCDPK2 (*left*) and NtCDPK3 (*right*) after infiltration of water as a mild stress stimulus (*B*) or after infiltration of 30 μM cantharidin (*C*).

RESULTS

NtCDPK2 and NtCDPK3 in Vivo Phosphorylation and Dephosphorylation Kinetics after Hypo-osmotic Stress

The *in vivo* phosphorylation of NtCDPK2 after biotic or abiotic stress results in an altered electrophoretic mobility of the kinase (21, 27). Here we show that HA-StrepII-tagged NtCDPK2 as well as NtCDPK3, transiently expressed in *N. benthamiana*, each display two electrophoretic mobility shifts after hypo-osmotic stress caused by the infiltration of water into the leaves (Fig. 1), suggesting that at least two distinct amino acids per kinase are subject to stress-dependent phosphorylation. In NtCDPK2, both mobility shifts were observed simultaneously within 1–2 min after stress (Fig. 1*A*, s2α and s2β). Such fast kinetics was seen for only one of the shifts of NtCDPK3 (s3α), whereas the second (s3β) appeared later between 8 and 16 min. Both kinases returned to their resting state within 2–4 h (Fig. 1*B*), which may be achieved either by proteolytic degradation of the phosphorylated CDPK coupled with *de novo* protein synthesis or by enzymatic dephosphorylation. Protein degradation was not observed because the overall amount of CDPK remained unchanged over time courses (Fig. 1*B*), even when *de novo* protein synthesis was inhibited by cycloheximide (not shown). However, the reversal of NtCDPK2

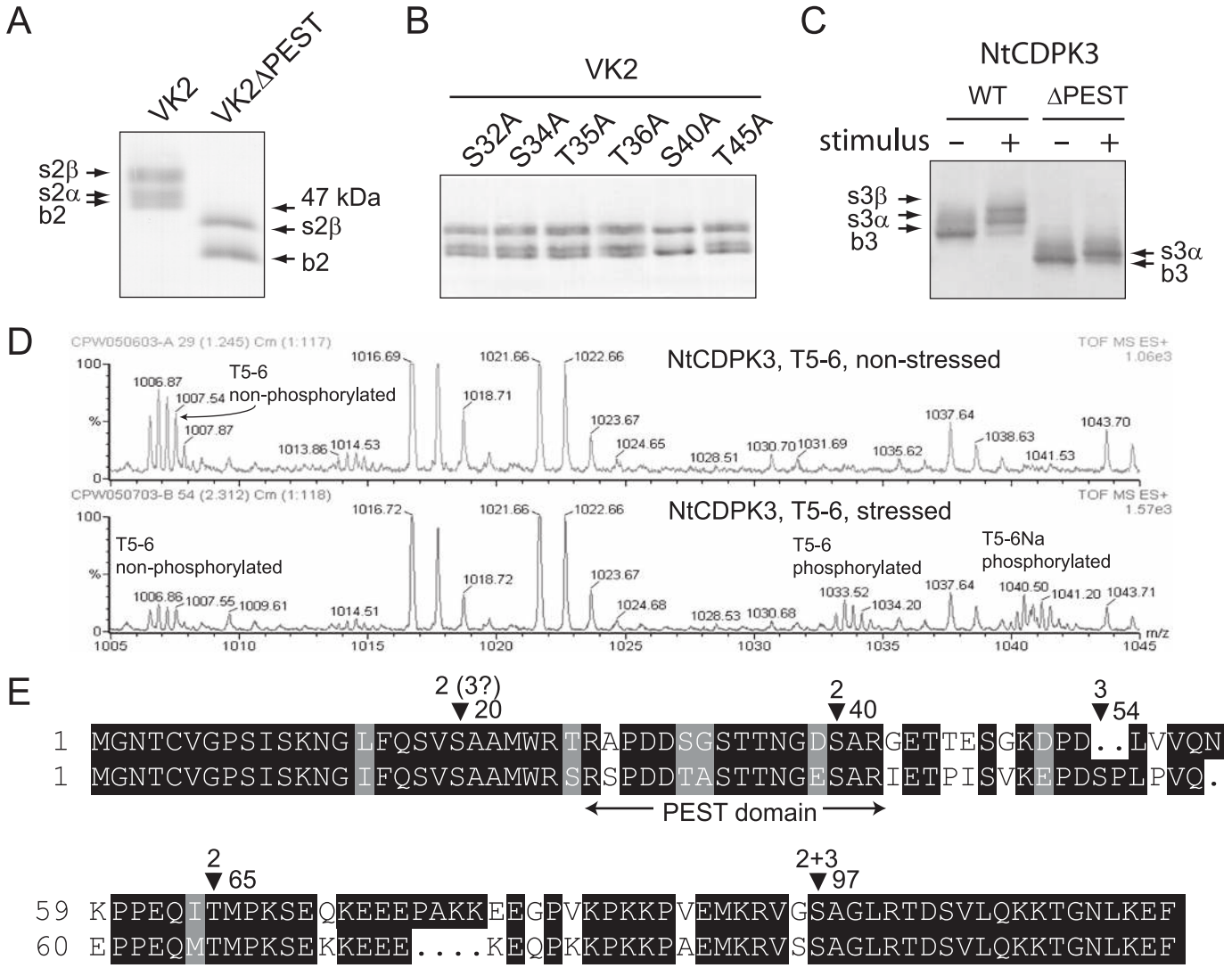

FIGURE 2. **Determination of phosphorylation sites for NtCDPK2 and NtCDPK3.** *A*, Western blots visualizing the shift pattern of truncated NtCDPK2-VK (*VK2*) and NtCDPK2-VK lacking the N-terminal PEST domain (*VK2ΔPEST*, lacking amino acids 27–42). *B*, as *A* for VK2 with individual alanine substitutions of all serine and threonine residues in the PEST domain. *C*, as *A* for stimulus-dependent shift pattern of NtCDPK3 (*WT*) and NtCDPK3 lacking the N-terminal PEST domain (Δ*PEST*; lacking amino acids 27–42). *D*, mass spectrum of tryptic digests of NtCDPK3 isolated from non-stressed (*top*) and stressed (*bottom*) leaves, respectively. *E*, alignment of the N termini of NtCDPK2 (*upper sequence*) and NtCDPK3. The positions of identified phosphorylation sites are indicated by *triangles*. The *number* indicates the corresponding CDPK.

and NtCDPK3 to the non-phosphorylated state was sensitive *in vivo* to the phosphatase inhibitor cantharidin (30 μM; Fig. 1*C*). For NtCDPK2, only one site was affected (corresponding to s2α), whereas dephosphorylation of both sites was affected in NtCDPK3. A complete shift of NtCDPK2 and NtCDPK3 into the s2α and s3β forms, respectively, was accomplished with 90 μM cantharidin after 2–4 h (not shown). The dose effect of phosphatase inhibitor on the phosphorylation status of the kinases suggests that phosphorylation and dephosphorylation are in a dynamic equilibrium. This may explain why several CDPK phosphorylation states can be observed *in vivo*.

Identification of in Vivo Phosphorylation Sites (P-sites) in NtCDPK2 and NtCDPK3

In truncated variants of NtCDPK2 and NtCDPK3 only containing the variable and kinase domains (VK2 and VK3), phosphorylation-dependent mobility shifts were still observed, indicating that the corresponding P-sites reside within these domains. Interestingly, phosphorylation became stimulus-independent in VK2 but not in VK3 (not shown). NtCDPK2 and NtCDPK3 contain a PEST domain in their N termini. Such domains were implicated in protein phosphorylation followed by protein degradation (33). A deletion of the 16-amino acid PEST domain in VK2 (amino acids 27–42) resulted in a lack of the phosphorylation shift s2α (Fig. 2*A*). An alanine scan of all possible P-sites within this region showed that phosphorylation at Ser^{40} is responsible for the s2α shift because it is absent in the S40A mutant enzyme (Fig. 2*B*). Thus, NtCDPK2 is phosphorylated *in vivo* at Ser^{40} in a stress-dependent manner, whereas other serines and threonines in the vicinity have no influence on this phosphorylation. A deletion of the PEST domain in NtCDPK3 (amino acids 27–42) resulted in a lack of s3β (Fig. 2*C*).

For a more general P-site search, we resorted to nanospray quadrupole time-of-flight MS. The kinases were isolated via the

StrepII tag (20) from unstressed and stressed leaves and prepared for MS. The resulting spectra were scanned for peptides that displayed the characteristic mass increase associated with phosphorylation. Tandem mass spectrometry was used to confirm and map phosphorylation sites. By comparing spectra from elicited and non-elicited kinase, we identified differential stress-dependent phosphorylation events. An example for NtCDPK3 is shown in Fig. 2*D*. Here peaks for the phosphorylated triply charged peptide T5-6 (amino acids 43–69; m/z 1033.18; sodiated form at m/z 1040.51) are only observed in the spectrum from the kinase isolated from an elicited leaf. The corresponding non-phosphorylated peptide (m/z 1006.51) is observed in both spectra, although it appears to be more abundant in the spectrum obtained from the unstressed leaf. From the four possible P-sites on peptide T5-6P (Thr^{45}, Ser^{48}, Ser^{54}, and Thr^{66}), only serine 54 was mapped as an exclusive site of modification by tandem MS analysis (supplemental Fig. S1). Ser^{54} represents an *in vivo* P-site in NtCDPK3 phosphorylated in a stimulus-dependent manner. Serine 54 is unique to NtCDPK3 and not present in NtCDPK2 (Fig. 2*E*).

In total, five *in vivo* phosphorylation sites were found in NtCDPK2 (supplemental Table S2; coverage 81.6%), and four *in vivo* sites were found in NtCDPK3 (supplemental Table S3; coverage 76.0%). We have used a variety of approaches to characterize these phosphorylations (see below and see "Experimental Procedures" for details), including the expression of kinase-inactive variants *in planta* to distinguish autophosphorylation from phosphorylation by different kinases and MS analysis of kinases expressed in *E. coli* (allowing only autophosphorylation). Most identified P-sites are located in the N terminus (Fig. 2*E*), whereas no modifications were found in the kinase and junction domains. The pattern of phosphorylation in the N terminus is different between both kinases despite an 82% amino acid identity in this region (overall, both kinases are 91% identical and 94% similar). The only common N-terminal phosphorylation site is serine 97 of NtCDPK2 (Ser^{94} in NtCDPK3; Fig. 2*E*). In NtCDPK3, phosphorylation at Ser^{20} was only observed after an *in vitro* autokinase reaction. This autophosphorylation is also present in the *Arabidopsis* orthologue AtCPK1 (17). A constitutive phosphorylation in the calmodulin-like domain at Ser^{572} (NtCDPK2) and Ser^{569} or Ser^{567} (NtCDPK3) has also been reported for AtCPK16 at Ser^{568} (17).

Characterization of Stress-inducible P-sites by Site-directed Mutagenesis

NtCDPK2—The altered electrophoretic mobility of the kinases as a result of phosphorylation may indicate significant structural changes that could be important in regulation. The wild-type enzyme of NtCDPK2 displayed two mobility shifts after stress (Fig. 3*A*, *lanes 1* and *2*), whereas the S40A and T65A variants lacked the lower (s2α; *lanes 3* and *4*) or upper shift (s2β; *lanes 5* and *6*). This demonstrates that Ser^{40} and Thr^{65} are phosphorylated independently of each other. The S40A/T65A double mutant lacked both shifts (*lanes 7* and *8*), whereas a phosphorylation mimic by S40D and T65D either in individual (not shown) or combined variants caused a constitutive shift (*lanes 9* and *10*).

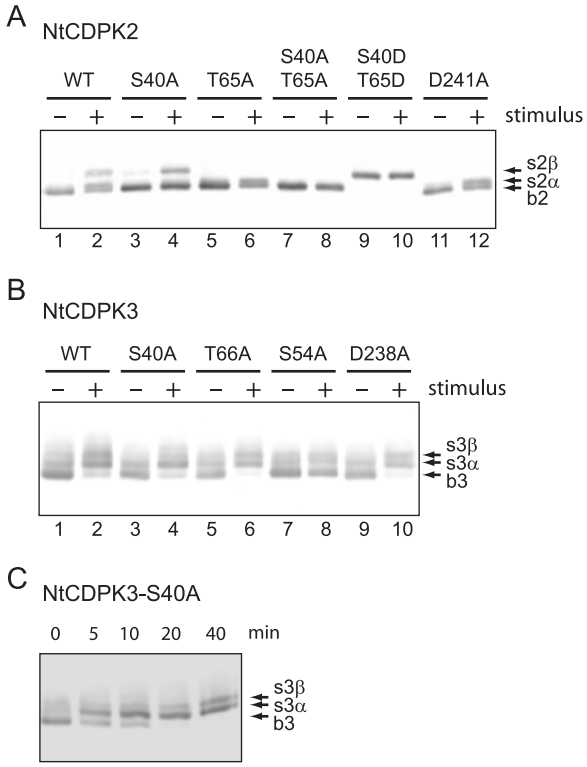

FIGURE 3. **Altered phosphorylation of NtCDPK2 and NtCDPK3 point mutants.** *A*, Western blot of NtCDPK2 before and 10 min after flooding stimulus. *B*, Western blot of NtCDPK3 before and 15 min after flooding stimulus. *C*, time course (on Western blot) after flooding stimulus for NtCDPK3-S40A mutant. The mobility shift s3β, corresponding to a phosphorylation in the PEST domain, is still observed but is delayed in this mutant.

NtCDPK3—For NtCDPK3, two shifts were observed within 15 min after stimulus (Fig. 3*B*, *lanes 1* and *2*). Introducing the mutation S40A (as identified in NtCDPK2) delayed but did not abolish the mobility shift s3β (Fig. 3, *B* (*lanes 3* and *4*) and *C*). Only a deletion of the complete PEST domain abolished s3β (Fig. 2*C*). Unfortunately, further fine mapping by MS (possible P-sites are Ser^{28}, Thr^{32}, Ser^{34}, Thr^{35}, Thr^{36}, and Thr^{45}) was not possible because the corresponding peptides were not observed in the spectra. Introducing the mutation T66A (corresponding to Thr^{65} auto-P-site responsible for s2β in NtCDPK2) had no impact on the mobility shifts (Fig. 3*B*, *lanes 5* and *6*). In addition, tandem MS analysis of peptide T5-6P (supplemental Fig. S1) comprising residue Thr^{66} clearly demonstrated exclusive stress-dependent phosphorylation at Ser^{54} and not Thr^{66}. Thus, despite nearly identical amino acid context around this threonine in both kinases (Fig. 2*E*), it is only accepted as an autophosphorylation site in NtCDPK2 and not in NtCDPK3. However, in AtCPK1, an *Arabidopsis* orthologue of NtCDPK2 and NtCDPK3, *in vitro* autophosphorylation at the corresponding threonine was observed (17). This demonstrates that for CDPKs, primary sequence conservation alone is not sufficient for P-site prediction. Introducing the mutation Ser^{54} had a strong effect on the NtCDPK3 shift pattern, leading to the lack of both stress-dependent mobility changes, s3α and s3β (Fig. 3*B*, *lanes 7* and *8*), whereas the PEST domain deletion mutant lacking amino acids 27–42 (thus containing Ser^{54}) still displayed s3α (Fig. 2*C*), appearing within 5 min after stress. In summary, our data suggest that phosphorylation at Ser^{54} cor-

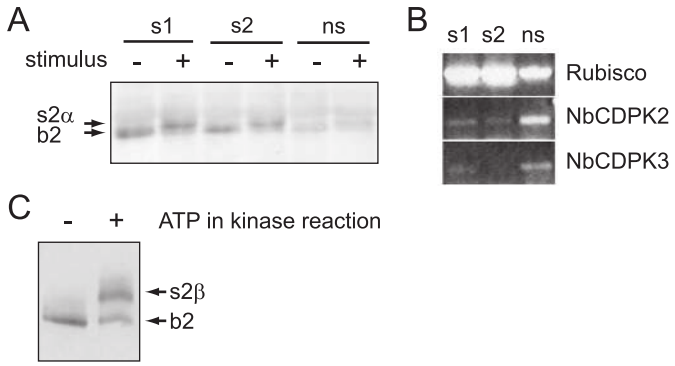

FIGURE 4. **Ser^{40} phosphorylation in NtCDPK2 is catalyzed by an upstream kinase.** *A*, Western blot of truncated kinase-inactive NtCDPK2-VK-D241A mutant before and 10 min after flooding stimulus. The construct was expressed in leaves of two independent plants silenced via the calmodulin-like domain for endogenous NbCDPK2 and NbCDPK3 (*s1* and *s2*) and in a non-silenced control plant (*ns*). *B*, reverse transcription-PCR demonstrating the effective silencing of NbCDPK2 and NbCDPK3. *C*, Western blot of purified NtCDPK2 from a non-elicited leaf subjected to a 15-min *in vitro* autokinase reaction without (−) and with (+) ATP.

responds to s3α and is a prerequisite for further timely delayed phosphorylation of the PEST domain corresponding to mobility shift s3β. In contrast to NtCDPK2, where phosphorylation events at Ser^{40} and Thr^{65} are independent of each other (Fig. 3*A*), *in vivo* phosphorylation in NtCDPK3 appears to follow a hierarchical order.

NtCDPK2 and NtCDPK3 were identified in plant defense signaling in a *Cf-9*/*Avr9* gene-for-gene interaction. Rapid NtCDPK2 phosphorylation was observed upon elicitation of *Cf-9* tobacco with AVR9 (21, 27). Therefore, we expressed StrepII-tagged NtCDPK2 and NtCDPK3 plus their variants with mutations in the identified phosphorylation sites transiently in *Cf-9* tobacco plants (*N. tabacum*) and investigated the phosphorylation pattern by Western blot after infiltration of intercellular fluid containing the fungal elicitor AVR9 into the apoplast. All NtCDPK2 and NtCDPK3 mobility shifts discussed above (and their absence when sites were blocked by mutation) observed in the *N. benthamiana* system after hypo-osmotic stress could be confirmed in *N. tabacum* in the context of the *Cf-9*/*Avr9* gene-for-gene interaction (data not shown).

Intramolecular NtCDPK2 Autophosphorylation at Thr^{65}

Non-elicited NtCDPK2 purified via the StrepII tag and subjected to an *in vitro* autokinase reaction displayed the form s2β (phosphorylation at Thr^{65}) but not s2α (phosphorylation at Ser^{40}; Fig. 4*C*). When a kinase-inactive variant of NtCDPK2 (mutant D241A) was expressed and the leaf was subjected to a stress stimulus, only s2α (phosphorylation at Ser^{40}) was observed, whereas s2β (phosphorylation at Thr^{65}) was absent (Fig. 3*A*, *lanes 11* and *12*). This identifies Thr^{65} (but not Ser^{40}) as an NtCDPK2 autophosphorylation site. In addition, it shows that Thr^{65} in NtCDPK2-D241A is not accepted for intermolecular autophosphorylation mediated by endogenous NbCDPK2 from *N. benthamiana*. *In planta* co-expression experiments of kinase-inactive NtCDPK2-D241A (HA-Strep-tagged) together with kinase-active NtCDPK2 (triple-Myc-tagged) confirmed that Thr^{65} autophosphorylation is an intramolecular reaction because the inactive variant was not phosphorylated in *trans* (supplemental Fig. S2). An alternative model fitting this data is that an unidentified intramolecular autophosphorylation event is required to make Thr^{65} accessible for phosphorylation.

NtCDPK2 Phosphorylation at Ser^{40}

In planta phosphorylation at Ser^{40} (s2α), in contrast to Thr^{65}, still occurs when the kinase-inactive NtCDPK2-D241A variant is expressed (Fig. 3*A*, *lanes 11* and *12*). This excludes an intramolecular autophosphorylation of the enzyme. We next investigated whether an intermolecular autophosphorylation mediated by endogenous NbCDPK2 may occur. In a combined reverse genetics approach, the closely related endogenous CDPKs in *N. benthamiana*, NbCDPK2 and NbCDPK3, were silenced by virus-induced gene silencing targeted to the calmodulin-like domain (21). Subsequently, a kinase-inactive truncated variant of NtCDPK2-VK-D241A lacking the targeted domain was expressed in the silenced leaves. In two NbCDPK-silenced plants, *in vivo* stress-dependent phosphorylation at Ser^{40} (s2α) could still be detected (Fig. 4*A*, *s1* and *s2*) like in a non-silenced control plant (*ns*). This documents that Ser^{40} of NtCDPK2 is phosphorylated by an unknown upstream kinase in response to a stress stimulus. Consistently, we never observed Ser^{40} phosphorylation in NtCDPK2 subjected to *in vitro* protein kinase reactions (Fig. 4*C*). Remarkably, Ser^{40} phosphorylation is constitutively present in the truncated NtCDPK2-VK2 variant (Fig. 2*A*) but only observed after elicitation in the corresponding kinase-inactive VK2-D241A mutant (Fig. 4*A*). These data suggest that NtCDPK2 activity feeds back on the kinase or phosphatase that regulates Ser^{40} phosphorylation and that the cell has no alternative means for CDPK inactivation when the regulatory CDPK domains are absent. Consistently, the active VK2 variant caused enhanced plant stress and defense responses in gain-of-function experiments even in the absence of elicitation (28).

NtCDPK3 Phosphorylation at Ser^{54} Only Occurs in Vivo

NtCDPK3 phosphorylation at Ser^{54} (possibly s3α) and within the PEST domain (possibly s3β) are probably catalyzed by an upstream kinase(s) because both shifts were detected in a kinase-inactive variant of NtCDPK3 (Fig. 3*B*, *lanes 9* and *10*), and MS analysis confirmed the presence of phosphorylated Ser^{54} in the kinase-inactive NtCDPK3 variant (not shown). In accordance, mobility shifts of the VK3 variant remained stimulus-dependent (not shown), although this truncated kinase can autophosphorylate constitutively. We purified NtCDPK3 from non-elicited and elicited leaves and subjected both preparations to an *in vitro* kinase reaction. Phosphorylation at Ser^{54} could not be generated *in vitro*, as indicated by the lack of the s3α mobility shift (supplemental Fig. S3) and by MS analysis (not shown). Similarly, PEST domain phosphorylation (s3β) was not observed *in vitro*. However, *in vitro* autophosphorylation caused a mobility shift never observed *in vivo* (supplemental Fig. S3), highlighting the potential risk of generating artifacts by *in vitro* kinase reactions often employed to map autophosphorylation sites. The data validate our approach to identify the *in vivo* phosphorylation pattern.

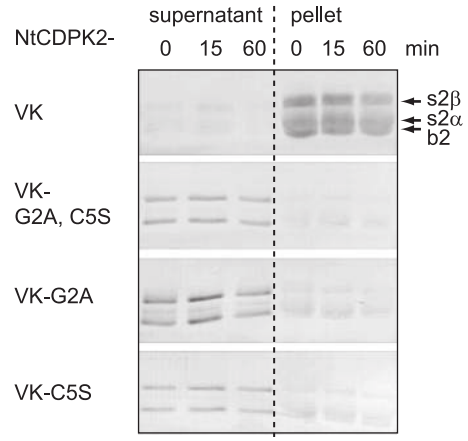

FIGURE 5. **Membrane association and phosphorylation of NtCDPK2 depends on myristoylation and palmitoylation motif.** Transiently expressed NtCDPK2-VK variants analyzed on Western blots before and at 15 and 60 min after flooding stimulus. *G2A*, putative myristoylation mutant; *C5S*, putative palmitoylation mutant. After ultracentrifugation of the extracts, only the VK2 form is found in the microsomal fraction (*pellet*) and is fully phosphorylated (*s2α* and *s2β*). The myristoylation and palmitoylation site mutants are found in the supernatant and lack the Ser^{40} phosphorylation (*s2α*).

The Phosphorylation Pattern Is Governed by the N-terminal Variable Domains

We next conducted domain swap experiments in which the N-terminal variable domains of NtCDPK2 (amino acids 1–116) and NtCDPK3 (amino acids 1–113) were mutually exchanged, generating two hybrid kinases NtCDPK2–3 and NtCDPK3–2 (supplemental Fig. S4). Upon transient expression in *N. benthamiana* and stress exposure, the phosphorylation patterns visualized by the shifts were identical to those of the CDPK from which the N-terminal domain originated and did not depend on the protein kinase domain present (supplemental Fig. S5). In agreement, in NtCDPK2-3 and NtCDPK3-2 hybrid variants, the mutations S40A and T65A (NtCDPK2) and S54A (NtCDPK3) compromised the corresponding phosphorylation shifts (not shown). These data suggest that structural constraints of the N termini determine the phosphorylation pattern independent from the kinase domain.

Membrane Localization Is Required for NtCDPK2 and NtCDPK3 Phosphorylation by Upstream Kinases

When the myristoylation or palmitoylation motif of NtCDPK2 was interrupted by introducing a G2A or C5S mutation, respectively, the kinase no longer remained associated with the microsomal pellet but was mainly located in the supernatant (Fig. 5). Remarkably, phosphorylation at Ser^{40} was lost in these acylation mutant variants. Correct subcellular membrane localization is therefore required for *in vivo* stimulus-dependent NtCDPK2 phosphorylation by the upstream kinase. A similar result was obtained for the NtCDPK3 (G2A) mutant, although partial Ser^{54} phosphorylation (but not PEST domain phosphorylation) was retained (not shown).

Impact of Phosphorylation Sites for NtCDPK2 in Vitro Kinase Activity

To elucidate whether the identified *in vivo* phosphorylation sites affect the enzyme activity of NtCDPK2 and NtCDPK3, wild-type enzymes and variants carrying site-specific mutations mimicking or blocking these phosphorylations were isolated from stressed leaves and were subjected to an *in vitro* kinase assay using syntide 2 as substrate. Kinase activity toward syntide 2 was not altered by the mutations (supplemental Fig. S6).

NtCDPK2 Function in Cell Death Response Requires Protein Kinase Activity and Membrane Localization

We could previously show that the expression of a truncated variant VK2 (but not VK3) resulted in enhanced plant defense responses in *N. benthamiana*, including the induction of hypersensitive response-like cell death symptoms (28). These responses were accelerated by a secondary mild abiotic stress stimulus. To test whether the identified phosphorylations affect NtCDPK2 *in vivo* function, we generated VK2 variants carrying amino acid substitutions that either block or mimic phosphorylation at S40A/T65A (VK2-AA) and S40D/T65D (VK2-DD), a delocalized variant VK2-G2A, and the kinase-inactive control VK2-D241A. These constructs were expressed in *N. benthamiana*, and leaves were assessed for the induction of cell death symptoms in the absence of any further stress stimulus by the autofluorescence of necrotic lesions (supplemental Fig. S7, *A* and *B*). In two biological replicates, each with 10 plants per construct, a loss of VK2-mediated cell death development was observed with the kinase-inactive VK2-D241A variant, and only weak symptoms developed with the delocalized variant. In contrast, slightly enhanced cell death symptoms were observed by the phosphorylation mimic VK2-DD variant and, remarkably, also by the variant VK2-AA. However, due to the large biological variance, the enhanced response of the phosphorylation mutants could at best be observed with marginal statistical significance (analysis of variance). These data show that kinase activity and correct membrane localization mediated by N-terminal acylation are required for biological function of NtCDPK2. Additionally, these results indicated that amino acid substitutions of Ser^{40} and Thr^{65} phosphorylated *in vivo* may alter NtCDPK2-dependent stress responses. This suggests that autophosphorylation and upstream kinase-mediated phosphorylation may be functionally important for stimulus-dependent CDPK regulation.

DISCUSSION

The mapping of *in vivo* P-sites performed in this study showed that NtCDPK2 and NtCDPK3 were almost exclusively phosphorylated in their respective N termini in a differential and stimulus-dependent manner. In addition, the phosphorylation patterns were determined by the respective N termini and not by the kinase domain, even in the case of autophosphorylations (supplemental Fig. S5). These data confirm the notion that specificity determinants of CDPKs are encoded within the variable N termini of these kinases (34).

We show that NtCDPK2 and NtCDPK3 are not only autophosphorylated but are also substrate to other (upstream)

protein kinases and therefore are components of protein kinase signaling cascades. Although calcium binding is a necessary prerequisite for CDPK activation, our data indicate that also kinase phosphorylation is mechanistically involved for the CDPK to become biologically functional. The phosphorylation of the NtCDPKs by unidentified upstream kinase(s) was observed to be stimulus-dependent (Fig. 1), suggesting that these kinases will also be activated during a biotic or abiotic stimulation. Additionally, the upstream kinases are probably membrane-associated because the corresponding phosphorylations were compromised when the membrane localization of the NtCDPKs was disturbed (Fig. 5). Potential candidates for CDPK-phosphorylating kinases may be found among the receptor-like kinases or the cytoplasmic kinases associated with membrane receptors (required, for example, in the case of the *Cf-9* disease resistance gene in the *Avr9*/*Cf-9* interaction (35)). Alternatively, members of the calcineurin B-like protein-interacting protein kinase/calcineurin B-like protein family may phosphorylate CDPKs. Membrane localization of calcineurin B-like protein-interacting protein kinases occurs via myristoylation and palmitoylation of the calcineurin B-like protein calcium sensors, which form stimulus-specific complexes with selected calcineurin B-like protein-interacting protein kinases (36, 37).

What is the functional role of CDPK phosphorylation? At our test conditions, full-length NtCDPK2 enzymes carrying specific amino acid substitutions at P-sites displayed no difference in phosphorylating activity toward the synthetic substrate syntide 2. However, it is possible that phosphorylation events so far unidentified are required for full enzyme activation. In other stress-related protein kinases (*e.g.* calcineurin B-like protein-interacting protein kinases or mitogen-activated protein kinases), phosphorylation occurs within the activation loop and causes an increase in kinase activity. Furthermore, CDPK phosphorylation may facilitate changes in the calcium binding affinity of the enzyme (*e.g.* allowing target substrate phosphorylation at lower calcium concentrations (24), rendering the enzyme in a sensitized state). Interestingly, exposure to a primary stimulus (incubation with abscisic acid) appears to leave guard cells in a status of enhanced calcium sensitivity (priming) for stomatal closure (38), and *Arabidopsis* CPK3 and CPK6 were shown to affect S-type anion channel activity in guard cells (11). One may speculate that CDPKs are part of a calcium-sensing regulatory circuit during ion channel regulation (39) and that the CDPK phosphorylation state (controlled by autophosphorylation and/or an upstream kinase) may be part of the postulated priming mechanism. Alternatively, phosphorylation could cause structural changes (as indicated by the electrophoretic mobility shifts) that may be a prerequisite to access and sequester *in vivo* phosphorylation targets (or to release them). Unfortunately, *in vivo* substrates for NtCDPK2 and NtCDPK3 are unknown.

A recent study also based on the *N. benthamiana* expression system identified plasma membrane NADPH-oxidase isoforms as targets for potato StCDPK4 and StCDPK5 (40). The ectopic expression of a truncated StCDPK5-VK variant resulted in an enhanced synthesis of reactive oxygen species in *N. benthamiana* leaves not observed in a variant lacking an intact myristoylation or palmitoylation motif. Like NtCDPK2, the potato CDPK may require correct localization for phosphorylation mediated by upstream kinases and to gain access to the target. However, unlike NtCDPK2-VK, StCDPK5-VK expression alone did not trigger cell death symptoms.

A mild stimulus (*e.g.* apoplast flooding) can accelerate cell death mediated by the VK2 variant but has no additional effect on VK2 phosphorylation at Ser^{40} and Thr^{65} (Fig. 5). Such a stimulus probably activates additional parallel signaling pathways, and the observed accelerated cell death may be the result of a concerted response reaction.

Our data suggest that the truncated gain-of-function variant NtCDPK2-VK (but not NtCDPK3-VK) feeds back on the upstream kinase (and/or phosphatase), causing a constitutive partial Ser^{40} (and Thr^{65}) phosphorylation and adopting a kinase-active conformation also in the absence of a stimulus (Figs. 2*A* and 5). Continuous CDPK signaling and finally cell death development are the result. These responses appear on average slightly enhanced in the phosphorylation mimic variant VK2-DD but also in variant VK2-AA (supplemental Fig. S7), although these changes could not be measured with statistical significance. Gain-of-function activities have also been reported for both the T271D and the T271A amino acid substitution at the autophosphorylation site in the calcium- and calmodulin-regulated protein kinase DMI3 from *Medicago truncatula*. Both variants resulted in functional proteins and were able to complement the *dmi3* mutant for nodulation development (41). Furthermore, a T265I substitution in the corresponding calcium- and calmodulin-regulated protein kinase protein from *Lotus japonicus* was identified as the causal mutation resulting in spontaneous nodulation of the *snf1* mutant (42). This indicates that phosphorylations do not only modulate protein properties by simply introducing a negative charge, and several functional models may be proposed in the case of NtCDPK2. (i) Phosphorylation may be required for effective kinase inactivation (*e.g.* by binding to an inhibitor). (ii) Structural changes in the N termini may alter the kinase binding affinity to the target(s). (iii) Binding affinity to other interactors (*e.g.* the upstream kinase) may be changed, reducing or enhancing the signal flux in feedback regulatory circuits.

The identification of *in vivo* phosphorylation sites is a crucial first step in understanding the regulation of CDPK function within a biological context. In the absence of tobacco mutant lines in *CDPK* genes, experiments in this report were based on gain-of-function analyses relying on ectopic expression *in planta*. Using cell death readout, this experimental system is at its limits for resolving altered biological responses of phosphorylation mutants that do not directly affect kinase activity. Currently, the number of reports in which *Arabidopsis* mutant lines in *CDPK* genes are linked to stress-related phenotypes is slowly increasing (10–12). Thus, future analysis of posttranslational modifications of CDPKs will probably include stable expression of kinase variants in the background of the corresponding mutant plants. The biological function of CDPK phosphorylation can then be addressed *in vivo* within the native signaling network triggering plant stress responses.

Acknowledgments—We acknowledge Frank Eickelmann, Bernd Richter, and Rainer Broz for excellent care and maintenance of plants.

REFERENCES

1. Hrabak, E. M., Chan, C. W., Gribskov, M., Harper, J. F., Choi, J. H., Halford, N., Kudla, J., Luan, S., Nimmo, H. G., Sussman, M. R., Thomas, M., Walker-Simmons, K., Zhu, J. K., and Harmon, A. C. (2003) *Plant Physiol.* **132,** 666–680
2. Chandran, V., Stollar, E. J., Lindorff-Larsen, K., Harper, J. F., Chazin, W. J., Dobson, C. M., Luisi, B. F., and Christodoulou, J. (2006) *J. Mol. Biol.* **357,** 400–410
3. Weljie, A. M., Gagné, S. M., and Vogel, H. J. (2004) *Biochemistry* **43,** 15131–15140
4. Yoo, B. C., and Harmon, A. C. (1996) *Biochemistry* **35,** 12029–12037
5. Harper, J. F., Huang, J. F., and Lloyd, S. J. (1994) *Biochemistry* **33,** 7267–7277
6. Harmon, A. C., Yoo, B. C., and McCaffery, C. (1994) *Biochemistry* **33,** 7278–7287
7. Böhmer, M., and Romeis, T. (2007) *Plant Mol. Biol.* **65,** 817–827
8. Harper, J. F., and Harmon, A. (2005) *Nat. Rev. Mol. Cell Biol.* **6,** 555–566
9. Cheng, S. H., Willmann, M. R., Chen, H. C., and Sheen, J. (2002) *Plant Physiol.* **129,** 469–485
10. Zhu, S. Y., Yu, X. C., Wang, X. J., Zhao, R., Li, Y., Fan, R. C., Shang, Y., Du, S. Y., Wang, X. F., Wu, F. Q., Xu, Y. H., Zhang, X. Y., and Zhang, D. P. (2007) *Plant Cell* **19,** 3019–3036
11. Mori, I. C., Murata, Y., Yang, Y. Z., Munemasa, S., Wang, Y. F., Andreoli, S., Tiriac, H., Alonso, J. M., Harper, J. F., Ecker, J. R., Kwak, J. M., and Schroeder, J. I. (2006) *PLoS Biol.* **4,** e327
12. Ma, S. Y., and Wu, W. H. (2007) *Plant Mol. Biol.* **65,** 511–518
13. Chehab, E. W., Patharkar, O. R., Hegeman, A. D., Taybi, T., and Cushman, J. C. (2004) *Plant Physiol.* **135,** 1430–1446
14. Glinski, M., Romeis, T., Witte, C. P., Wienkoop, S., and Weckwerth, W. (2003) *Rapid Commun. Mass Spectrom.* **17,** 1579–1584
15. Hegeman, A. D., Harms, A. C., Sussman, M. R., Bunner, A. E., and Harper, J. F. (2004) *J. Am. Soc. Mass Spectrom.* **15,** 647–653
16. Rutschmann, F., Stalder, U., Piotrowski, M., Oecking, C., and Schaller, A. (2002) *Plant Physiol.* **129,** 156–168
17. Hegeman, A. D., Rodriguez, M., Han, B. W., Uno, Y., Phillips, G. N., Jr., Hrabak, E. M., Cushman, J. C., Harper, J. F., Harmon, A. C., and Sussman, M. R. (2006) *Proteomics* **6,** 3649–3664
18. de la Fuente van Bentem, S., Anrather, D., Dohnal, I., Roitinger, E., Csaszar, E., Joore, J., Buijnink, J., Carreri, A., Forzani, C., Lorkovic, Z. J., Barta, A., Lecourieux, D., Verhounig, A., Jonak, C., and Hirt, H. (2008) *J. Proteome Res.* **7,** 2458–2470
19. Nühse, T. S., Stensballe, A., Jensen, O. N., and Peck, S. C. (2004) *Plant Cell* **16,** 2394–2405
20. Witte, C. P., Noël, L. D., Gielbert, J., Parker, J. E., and Romeis, T. (2004) *Plant Mol. Biol.* **55,** 135–147
21. Romeis, T., Ludwig, A. A., Martin, R., and Jones, J. D. (2001) *EMBO J.* **20,** 5556–5567
22. Chaudhuri, S., Seal, A., and Gupta, M. D. (1999) *Plant Physiol.* **120,** 859–866
23. Bögre, L., Olah, Z., and Dudits, D. (1988) *Plant Sci.* **58,** 135–144
24. Lee, J. Y., Yoo, B. C., and Harmon, A. C. (1998) *Biochemistry* **37,** 6801–6809
25. Hudmon, A., and Schulman, H. (2002) *Annu. Rev. Biochem.* **71,** 473–510
26. Soderling, T. R. (1999) *Trends Biochem. Sci.* **24,** 232–236
27. Romeis, T., Piedras, P., and Jones, J. D. (2000) *Plant Cell* **12,** 803–816
28. Ludwig, A. A., Saitoh, H., Felix, G., Freymark, G., Miersch, O., Wasternack, C., Boller, T., Jones, J. D., and Romeis, T. (2005) *Proc. Natl. Acad. Sci. U.S.A.* **102,** 10736–10741
29. Weiner, M. P., Costa, G. L., Schoettlin, W., Cline, J., Mathur, E., and Bauer, J. C. (1994) *Gene* **151,** 119–123
30. Horton, R. M., Hunt, H. D., Ho, S. N., Pullen, J. K., and Pease, L. R. (1989) *Gene* **77,** 61–68
31. Yoon, G. M., Dowd, P. E., Gilroy, S., and McCubbin, A. G. (2006) *Plant Cell* **18,** 867–878
32. Voinnet, O., Rivas, S., Mestre, P., and Baulcombe, D. (2003) *Plant J.* **33,** 949–956
33. Rechsteiner, M., and Rogers, S. W. (1996) *Trends Biochem. Sci.* **21,** 267–271
34. Harmon, A. C., Gribskov, M., Gubrium, E., and Harper, J. F. (2001) *New Phytol.* **151,** 175–183
35. Van der Biezen, E. A., and Jones, J. D. (1998) *Trends Biochem. Sci.* **23,** 454–456
36. Batistic, O., and Kudla, J. (2009) *Biochim. Biophys. Acta* **1793,** 985–992
37. Batistic, O., Sorek, N., Schültke, S., Yalovsky, S., and Kudla, J. (2008) *Plant Cell* **20,** 1346–1362
38. Siegel, R. S., Xue, S., Murata, Y., Yang, Y., Nishimura, N., Wang, A., and Schroeder, J. I. (2009) *Plant J.* **59,** 207–220
39. Young, J. J., Mehta, S., Israelsson, M., Godoski, J., Grill, E., and Schroeder, J. I. (2006) *Proc. Natl. Acad. Sci. U.S.A.* **103,** 7506–7511
40. Kobayashi, M., Ohura, I., Kawakita, K., Yokota, N., Fujiwara, M., Shimamoto, K., Doke, N., and Yoshioka, H. (2007) *Plant Cell* **19,** 1065–1080
41. Gleason, C., Chaudhuri, S., Yang, T., Muñoz, A., Poovaiah, B. W., and Oldroyd, G. E. (2006) *Nature* **441,** 1149–1152
42. Tirichine, L., Imaizumi-Anraku, H., Yoshida, S., Murakami, Y., Madsen, L. H., Miwa, H., Nakagawa, T., Sandal, N., Albrektsen, A. S., Kawaguchi, M., Downie, A., Sato, S., Tabata, S., Kouchi, H., Parniske, M., Kawasaki, S., and Stougaard, J. (2006) *Nature* **441,** 1153–1156